Inorg. Chem. **2006**, *45*, 4974–4981

Density Functional Theory Study of 10-Atom Germanium Clusters: Effect of Electron Count on Cluster Geometry

R. B. King,*,† I. Silaghi-Dumitrescu,‡ and M. M. Uţă‡

Department of Chemistry, University of Georgia, Athens, Georgia 30602, and Faculty of Chemistry and Chemical Engineering, Babeş-Bolyai University, Cluj-Napoca, Roumania

Received November 3, 2005

Density functional theory (DFT) at the hybrid B3LYP level has been applied to Ge_{10}^{z} germanium clusters ($z = -6$, -4, -2, 0, +2, +4, +6) starting from 12 different initial configurations. The D_{4d} 4,4-bicapped square antiprism found experimentally in $B_{10}H_{10}^{2-}$ and other 10-vertex clusters with 22 skeletal electrons is calculated for the isoelectronic Ge_{10}^{2-} to be the global minimum by more than 15 kcal/mol. The global minima found for electron-rich clusters Ge_{10}^{4-} and Ge_{10}^{6-} are not those known experimentally. However, experimentally known structures for *nido*-$B_{10}H_{14}$ and the pentagonal antiprism of *arachno*-Pd@Bi_{10}^{4+} are found at higher but potentially accessible energies for Ge_{10}^{4-} and Ge_{10}^{6-}. The global minimum for Ge_{10} is the C_{3v} 3,4,4,4-tetracapped trigonal prism predicted by the Wade–Mingos rules and found experimentally in isoelectronic Ni@Ga_{10}^{10-}. However, only slightly above this global minimum for Ge_{10} (+3.3 kcal/mol) is the likewise C_{3v} *isocloso* 10-vertex deltahedron found in metallaboranes such as (η^6-arene)RuB_9H_9 derivatives. Structures found for more electron-poor clusters Ge_{10}^{2+} and Ge_{10}^{4+} include various capped octahedra and pentagonal bipyramids. This study predicts a number of 10-vertex cluster structures that have not yet been realized experimentally but would be interesting targets for future synthetic 10-vertex cluster chemistry using vertex units isolobal with the germanium vertices used in this work.

1. Introduction

Previous papers from our group discuss our results from density functional theory (DFT) computations on six-vertex atom clusters of the group 13 elements boron, indium, and thallium[1,2] and on five-,[3] six-,[3] seven-,[3] eight, [4] nine-,[5] and 11-atom[6] germanium clusters. We have now extended such calculations to 10-atom germanium clusters. Ten-atom clusters are of interest for the following reasons:

(1) A variety of 10-vertex cage boranes[7] are known, including *closo* derivatives, as exemplified by $B_{10}H_{10}^{2-}$ [8,9] and isoelectronic carboranes; *nido* derivatives such as $B_{10}H_{14}$;[10] *arachno* derivatives such as $B_{10}H_{14}^{2-}$;[11] and *isocloso* derivatives such as (η^6-arene)RuB_9H_9.[12]

(2) Some 10-vertex metal carbonyl clusters are known, such as bicapped square antiprismatic $[Co_{10}(\mu_8\text{-P})(CO)_{22}]^{3-}$ [13] and tetracapped octahedral $Os_{10}H_4(CO)_{24}^{2-}$.[14]

(3) No empty 10-vertex Zintl ions are known, but examples of filled interstitial 10-vertex Zintl ions include 3,4,4,4-tetracapped trigonal prismatic Ni@Ga_{10}^{10-} [15] and pentagonal antiprismatic Pd@Bi_{10}^{4+}.[16]

* To whom correspondence should be addressed. E-mail: rbking@sunchem.uga.edu.

† University of Georgia.

‡ Babeş-Bolyai University.

(1) King, R. B.; Silaghi-Dumitrescu, I.; Kun, A. *Inorg. Chem.* **2001**, *40*, 2450.
(2) King, R. B.; Silaghi-Dumitrescu, I.; Kun, A. In *Group 13 Chemistry: From Fundamentals to Applications*; Shapiro, P., Atwood, D. A., Eds.; American Chemical Society: Washington, DC, 2002; pp 208−225.
(3) King, R. B.; Silaghi-Dumitrescu, I.; Kun, A. *Dalton Trans.* **2002**, 3999.
(4) King, R. B.; Silaghi-Dumitrescu, I.; Lupan, A. *Dalton Trans*. **2005**, 1858.
(5) King, R. B.; Silaghi-Dumitrescu, I. *Inorg. Chem*. **2003**, *42*, 6701.
(6) King, R. B.; Silaghi-Dumitrescu, I.; Lupan, A. *Inorg. Chem.* **2005**, *44*, 3579.
(7) Muetterties, E. L. *Boron Hydride Chemistry*; Academic Press: New York, 1975.
(8) Dobrott, R. D.; Lipscomb, W. N. *J. Chem. Phys*. **1962**, *37*, 1779.
(9) Hofmann, K.; Albert, B. *Z. Naturforsch.* **2000**, *55b*, 499.
(10) Kasper, J. S.; Lucht, C. M.; Harker, D. *Acta Crystallogr.* **1950**, *3*, 436.
(11) Lipscomb, W. N.; Wiersema, R. J.; Hawthorne, M. F. *Inorg. Chem.* **1972**, *11*, 651.
(12) Kim, Y.; Cooke, P. A.; Rath, N. P.; Barton, L.; Greatrex, R.; Kennedy, J. D.; Thornton-Pett, M. *Inorg. Chem. Commun.* **1998**, *1*, 375.
(13) Ciani, G.; Sironi, A.; Martinengo, S.; Garlaschelli, L.; Della Pergola, R.; Zanello, P.; Laschi, F.; Masciocchi, N. *Inorg. Chem.* **2001**, *40*, 3905.
(14) Braga, D.; Lewis, J.; Johnson, B. F. G.; McPartlin, M.; Nelson, W. J. H.; Vargas, M. D. *Chem. Commun*. **1983**, *241*.
(15) Henning, R. W.; Corbett, J. D. *Inorg. Chem.* **1999**, *38*, 3883.
(16) Ruck, M.; Dubenskyy, V.; Söhnel, T. *Angew. Chem., Int. Ed.* **2003**, *43*, 2978.

10.1021/ic051905m CCC: $33.50 © 2006 American Chemical Society
Published on Web 05/25/2006

Experimental work in these areas suggests a considerable variety in the 10-vertex polyhedra found in the cluster structures depending on the skeletal-electron count.

The objective of the research discussed in this paper is to extend our DFT studies to 10-vertex cluster structures in order to continue our study on the effects of electron count on cluster geometry. As before,[4,6] germanium clusters Ge_{10}^{z} ($z = -6, -4, -2, 0, +2, +4, +6$) were chosen as tractable systems with vertices isolobal to the various types of vertices found in 10-atom inorganic clusters, including boranes and metallaboranes, metal carbonyl clusters, and post-transition element clusters (e.g., Zintl ions). The range of charges on Ge_{10}^{z} chosen for this work spans the 26 skeletal electrons required for an *arachno* 10-vertex cluster ($26 = 2n + 6$ for $n = 10$), i.e., Ge_{10}^{6-}, to 14 skeletal electrons in Ge_{10}^{6+}. Furthermore, the choice of germanium as the vertex atom for this study of 10-vertex clusters minimizes the maximum charge required for the range of 26−14 skeletal electrons in 10-vertex clusters with bare vertex atoms. Isoelectronic and isolobal relationships provide analogies of our computational results on Ge_{10}^{z} clusters to experimentally known borane, metal carbonyl, and Zintl ion structures.

2. Computational Methods

Geometry optimizations were carried out at the hybrid DFT B3LYP level[17] with the 6-31G(d) (valence) double-ζ quality basis functions extended by adding one set of polarization (d) functions. The Gaussian 94 package of programs[18] was used, in which the fine grid (75 302) is the default for numerically evaluating the integrals and the tight (1×10^{-8}) hartree stands as a default for the self-consistent field convergence. Computations were carried out using 12 initial geometries, including examples of 10-vertex polyhedra with 3-, 4-, and 5-fold symmetry (see the Supporting Information). The symmetries were maintained during the geometry optimization processes. In addition, symmetry breaking using modes defined by imaginary vibrational frequencies was used to determine optimized structures with minimum energies. Vibrational analyses show that all of the final optimized structures discussed in this paper are genuine minima at the B3LYP/6-31G(d) level without any significant imaginary frequencies. In a few cases, particularly for some of the hypoelectronic structures, the calculations ended with acceptable small imaginary frequencies, and these values are indicated in the corresponding figures.[19]

Archibong and St-Anant[20] have found that B3LYP and CCSD(T) results on Ge_6^{z} ($z = 0, -1$) clusters are in reasonable agreement, so no further test on the reliability of the B3LYP method was undertaken in this work. The effect of the environment on the relative stability of Ge_n^{z-} clusters has been considered[5] by placing the countercharges on the Connolly surface of the system. B3LYP calculations in the field of such charges showed no change in the order of the energies of the calculated isomers. Moreover, CPCM SCRF calculations[21] in tetrahydrofuran (THF) on the $Ge_{10}^{(-2,-4,-6)}$ clusters also confirm that the gas-phase global minima remain global minima in solution (see ref 22 for a similar problem in polyoxometalate chemistry).

The optimized structures found for the Ge_{10}^{z} clusters are summarized in Figures 1−6 (relative energies in kcal/mol). To distinguish between the large number of structures, we labeled them by the number of skeletal electrons and relative energies. Thus the lowest-energy structure with 22 skeletal electrons (i.e., Ge_{10}^{2-}) is designated as **22−1**. The letter "T" is used to designate triplet structures. More details of all of the optimized structures, including all interatomic distances and the initial geometries leading to a given optimized structure, are provided in the Supporting Information.

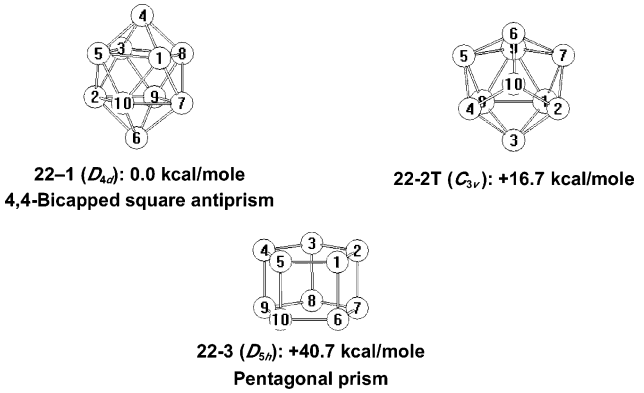

Figure 1. Three lowest-energy optimized structures for Ge_{10}^{2-}.

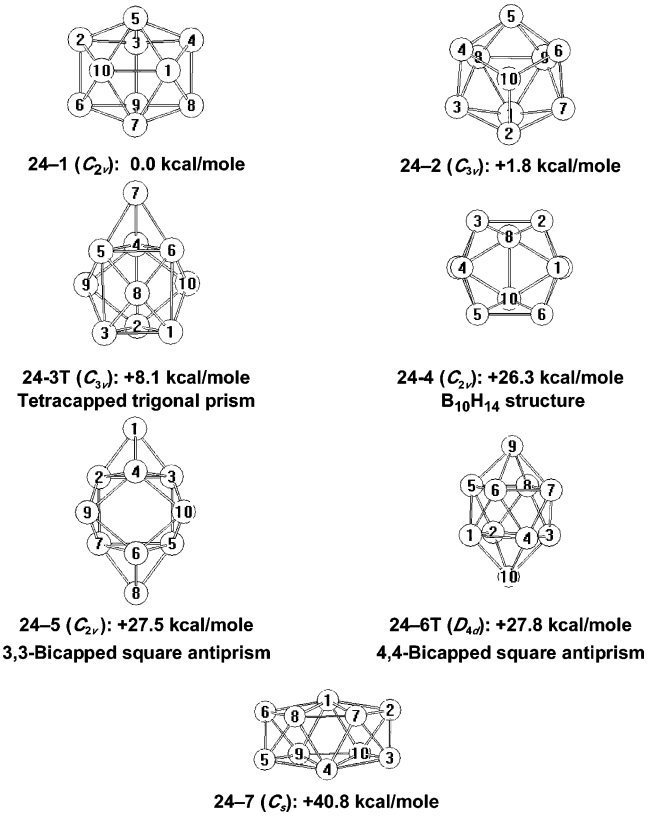

Figure 2. Seven lowest-energy optimized structures for Ge_{10}^{4-}.

(17) Becke, A. D. *J. Chem. Phys.* **1993**, *98*, 5648.
(18) Frisch, M. J.; Trucks, G. W.; Schlegel, H. B.; Gill, P. M. W.; Johnson, B. G.; Robb, M. A.; Cheeseman, J. R.; Keith, T.; Petersson, G. A.; Montgomery, J. A.; Raghavachari, K.; Al-Laham, M. A.; Zakrzewski, V. G.; Ortiz, J. V.; Foresman, J. B.; Peng, C. Y.; Ayala, P. Y.; Chen, W.; Wong, M. W.; Andres, J. L.; Replogle, E. S.; Gomperts, R.; Martin, R. L.; Fox, D. J.; Binkley, J. S.; Defrees, D. J.; Baker, J.; Stewart, J. J. P.; Head-Gordon, M.; Gonzalez, C.; Pople, J. A. *Gaussian 94*, revision C.3; Gaussian, Inc.: Pittsburgh, PA, 1995.
(19) Xie, Y.; Schaefer, H. F., III; King, R. B. *J. Am. Chem. Soc.* **2000**, *122*, 8746.
(20) Archibong, E. F.; St-Amant, A. *J. Chem. Phys.* **1998**, *109*, 962.
(21) Klamt, A.; Schüürmann, G. *J. Chem. Soc., Perkin Trans. 2* **1993**, 799.
(22) López, X.; Fernández, J. A.; Romo, S.; Paul, J. F.; Kazansky, L.; Poblet, J. M. *J. Comput. Chem.* **2004**, *25*, 1542.

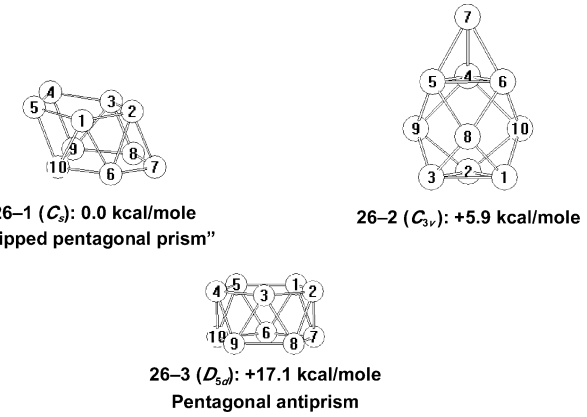

Figure 3. Three lowest-energy optimized structures for Ge_{10}^{6-}.

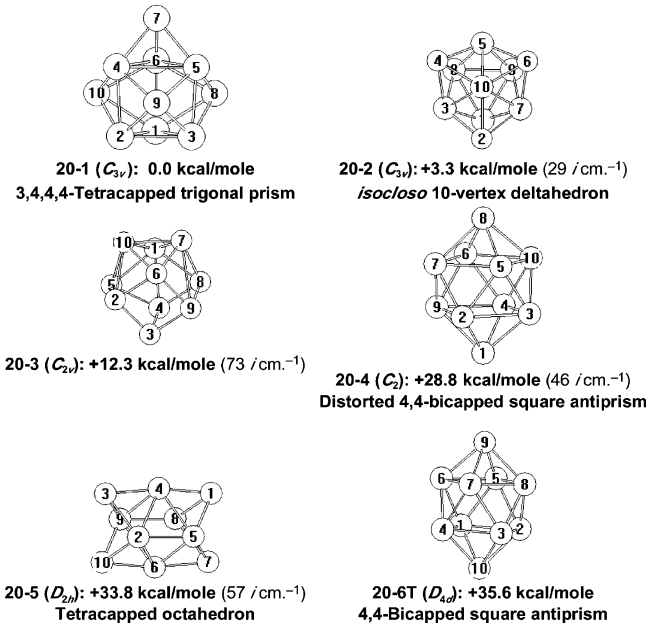

Figure 4. Six lowest-energy optimized structures for Ge_{10}.

In assigning polyhedra to the optimized structures, we normally considered Ge−Ge distances less than ~3.25 Å as polyhedral edges.

For the most highly charged structures ($Ge_{10}^{\pm 6}$), the lowest-energy optimized configurations involved fragmentation of the eight-vertex cluster into smaller units. Only structures in which the 10 germanium vertices remain connected are considered.

3. Results

3.1. Twenty-Two Skeletal Electron Ge_{10}^{2-} (Figure 1). The D_{4d} bicapped square antiprism structure **22−1** was found to be the global minimum, consistent with the experimental observation that this is the favored structure for most 22-skeletal-electron clusters, including $B_{10}H_{10}^{2-}$ [8,9] and $Co_{10}(\mu_8\text{-P})(CO)_{22}^{3-}$,[13] in accord with the Wade−Mingos rules.[23−26] The next higher-lying structure for Ge_{10}^{2-} at +16.7 kcal/mol was the C_{3v} *isocloso* structure **22−2T**, found to be a triplet, consistent with the experimental observation of singlet *isocloso* structures for metallaboranes such as (η^6-arene)-RuB_9H_9 derivatives with 20 rather than 22 skeletal electrons. Thus, the triplet multiplicity of **22−2T** is consistent with a half-filled doubly degenerate frontier HOMO. The next higher-lying structure for Ge_{10}^{2-}, **22−3**, is a D_{5h} pentagonal prismatic structure lying +40.7 kcal/mol above the global minimum.

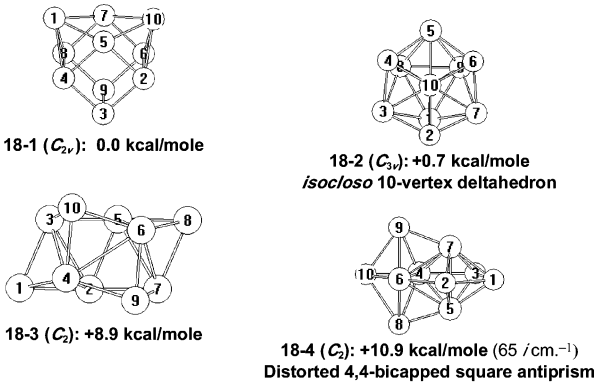

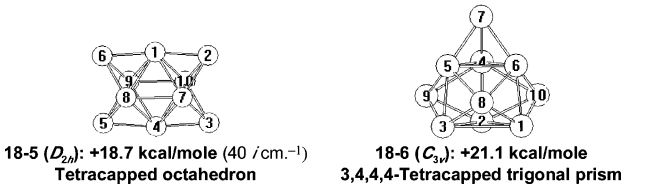

Figure 5. Six lowest-energy optimized structures for Ge_{10}^{2+}.

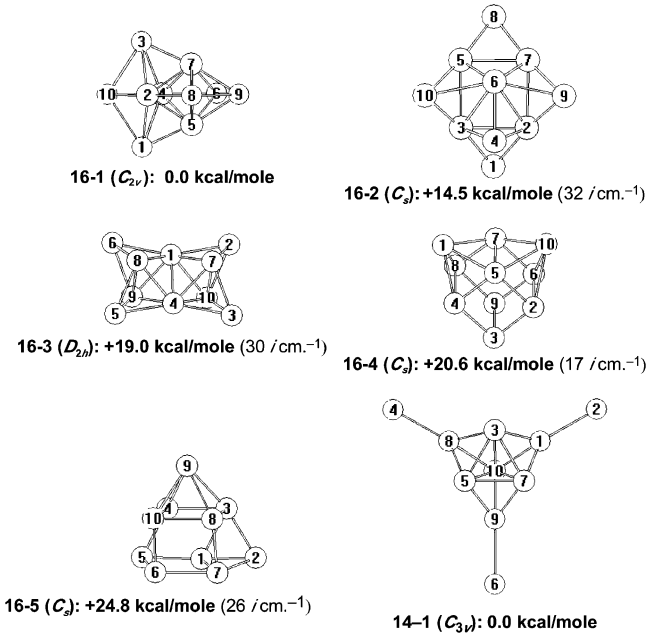

Figure 6. Five lowest-energy optimized structures for Ge_{10}^{4+} and the single connected structure (**14−1**) found for Ge_{10}^{6+}.

3.2. Hyperelectronic Structures. The global minimum for Ge_{10}^{4-} (Figure 2) is not the C_{2v} *nido* structure with an open hexagonal face found experimentally[10] for the relatively stable $B_{10}H_{14}$ but instead a related C_{2v} structure, **24−1**, in which the hexagonal face of $B_{10}H_{14}$ has been replaced by two quadrilateral faces. The $B_{10}H_{14}$ type structure **24−4** was also found for Ge_{10}^{4-} but at +26.3 kcal/mol above the global minimum. Between these two structures was found the *isocloso* structure **24−2**, at +1.8 kcal/mol above the global

(23) Wade, K. *Chem. Commun.* **1971**, 792.
(24) Wade, K. *Adv. Inorg. Chem. Radiochem.* **1976**, *18*, 1.
(25) Mingos, D. M. P. *Nature Phys. Sci.* **1972**, *99*, 236.
(26) Mingos, D. M. P. *Acc. Chem. Res.* **1984**, *17*, 311.

minimum, and the triplet C_{3v} tetracapped trigonal prism structure **24**−**3T**, at +8.1 kcal/mol above the global minimum. Higher-energy structures for Ge_{10}^{4-} include the C_{2v} 3,3-bicapped square antiprism **24**−**5**, the D_{4d} 4,4-bicapped square antiprism **24**−**6T**, and a novel oblate deltahedral structure **24**−**7** derived by edge-sharing fusion of two octahedra followed by lengthening the edge common to both octahedra. The deltahedron in structure **24**−**7** has two degree 6 vertices, in contrast to the single degree 6 vertex in the *isocloso* structure and no degree 6 vertices in the most-spherical 4,4-bicapped square antiprism (e.g., structures **22**−**1** and **24**−**6T**).

The cluster Ge_{10}^{6-}, with an *arachno* electron count of 26 = $2n + 6$ for $n = 10$, has only three structures within 25 kcal/mol of the global minimum (Figure 3). The D_{5d} pentagonal antiprism **26**−**3**, anticipated by the Wade−Mingos rules[23−26] for an *arachno* 10 vertex structure and found experimentally in $Pd@Bi_{10}^{4+}$, is +17.1 kcal/mol above the C_s global minimum **26**−**1**, which also has two pentagonal faces. Structure **26**−**1** is derived from a pentagonal prism by sliding the top pentagon relative to the bottom pentagon to make three of the five rectangular faces of the original pentagonal prism into pairs of triangles. The resulting polyhedron in **26**−**1** thus has two pentagonal faces, two quadrilateral faces, and six triangular faces. The C_{3v} structure **26**−**2**, intermediate in energy between structures **26**−**1** and **26**−**3**, is derived from the nine-vertex most-spherical deltahedron, namely the 4,4,4-tricapped trigonal prism, by the following sequence of processes:

(1) The 4,4,4-tricapped trigonal prism is stretched along its C_3 axis so that the vertical edges of the underlying trigonal prism are no longer edges and the resulting polyhedron can be regarded as a nine-vertex *hypho* polyhedra with the anticipated *hypho* 26 skeletal-electron count (26 = $2n + 8$ for $n = 9$). This nine-vertex *hypho* polyhedron has all degree 4 vertices and is the third smallest polyhedron with all degree 4 vertices, after the O_h octahedron and the D_{4d} square antiprism with six and eight vertices, respectively.

(2) Capping one of the remaining two triangular faces to reduce the overall symmetry from D_{3h} to C_{3v}.

The resulting polyhedron in **26**−**2** thus may be regarded as a 3-capped *hypho* polyhedron, thereby combining the open (nontriangular) faces of hyperelectronic polyhedra with the capped triangular faces (i.e., tetrahedral cavities) of hypoelectronic polyhedra. The $2n + 6$ skeletal-electron count in structure **26**−**2** for Ge_{10}^{6-} is in accord with the Wade−Mingos rules,[23−26] because the single capped triangular face in **26**−**2** neutralizes one of the three quadrilateral faces of the underlying nine-vertex *hypho* polyhedron, leading to an anticipated *arachno* electron count for the complete 10-vertex structure.

3.3. The Neutral Ge_{10} (Figure 4). A neutral Ge_{10} cluster is certainly unstable with respect to polymerization to bulk germanium metal. However, computations on neutral Ge_{10} are of interest in order to characterize the relative stabilities of various 10-vertex polyhedra in 20-skeletal-electron systems such as *isocloso* metallaboranes exemplified by (η^6-arene)RuB_9H_9.[12] The skeletal bonding in (η^6-arene)RuB_9H_9 and related *isocloso* metallaboranes has been interpreted[27] as consisting of 3c−2e bonds in 10 of the 16 faces of the deltahedron.

The global minimum for Ge_{10} is the C_{3v} tetracapped trigonal prism **20**−**1**. This can be derived by capping one of the faces of the D_{3h} tricapped trigonal prism, which is the most spherical nine-vertex deltahedron and is thus expected to have 20 = (2)(9) + 2 skeletal electrons by the Wade−Mingos rules. As is usual for such hypoelectronic polyhedra, the cap on the triangular face leading to a tetrahedral cavity contributes its skeletal electrons but no skeletal bonding orbitals. This polyhedron is found in the structurally characterized[15] $Ni@Ga_{10}^{10-}$. If the interstitial Ni atom in $Ni@Ga_{10}^{10-}$ is assumed to be a donor of zero skeletal electrons in accord with its filled d^{10} shell,[28] then $Ni@Ga_{10}^{10-}$ is isoelectronic with neutral Ge_{10}.

The C_{3v} 10-vertex *isocloso* deltahedron **20**−**2**, found experimentally in metallaboranes such as (η^6-arene)RuB_9H_9 mentioned above, lies only + 3.3 kcal/mol above the global minimum **20**−**1**. The next highest-lying structure, namely C_{2v} **20**−**3** at + 12.3 kcal/mol, is derived from a C_{2v} bicapped cube by bringing the two caps close enough to each other to make a new edge of comparable length to that of the underlying cube.

Two of the higher-lying structures energetically found for neutral Ge_{10} are derived from the 4,4-bicapped square antiprism that is the global minimum for Ge_{10}^{2-} (**22**−**1**) through the loss of two skeletal electrons. The singlet structure of this type (**20**−**4**) at +28.8 kcal/mol above the global minimum **20**−**1** is distorted from D_{4d} symmetry to C_2 symmetry, an apparent manifestation of the Jahn−Teller effect. A higher-lying triplet 4,4-bicapped square antiprism for Ge_{10} (**20**−**6T**) at +35.6 kcal/mol above the global minimum retains D_{4d} symmetry. The one other Ge_{10} isomer found within 40 kcal/mol of the global minimum **20**−**1** is the tetracapped octahedron **20**−**5** of approximate D_{2h} symmetry at +33.8 kcal/mol above global minimum **20**−**1**.

3.4. Other Hypoelectronic Structures. A number of distinct minima were found for the Ge_{10}^{2+} dication; the six rather unusual structures within 25 kcal/mol of the global minimum are depicted in Figure 5. None of these structures have yet been realized experimentally.

The lowest-lying structure for Ge_{10}^{2+}, **18**−**1**, is a C_{2v} bicapped cube. In this structure, eight of the 10 germanium atoms form two square pyramids sharing an edge. The next higher-lying structure at only 0.7 kcal/mol above the global minimum is the *isocloso* type C_{3v} structure **18**−**2**, which is similar to **20**−**2** for the 20-skeletal-electron Ge_{10}.

The next higher-lying structure for Ge_{10}^{2+}, **18**−**3**, at +8.9 kcal/mol is an unfamiliar C_2 10-vertex polyhedron with four vertices of degree 3, four vertices of degree 5, and two vertices of degree 6. Two of the faces are irregular quadrilaterals, and the remaining 12 faces are triangles. Two of the degree 3 vertices cap triangular faces of an underlying eight-vertex polyhedron, leading to tetrahedral cavities; the

(27) King, R. B. *Inorg. Chem.* **1999**, *38*, 5151.
(28) King, R. B. *Dalton Trans.* **2004**, 3420.

other two degree 3 vertices do not function as such caps. This rather twisted polyhedron is chiral, in accord with its C_2 point group.

The next higher-lying structure for Ge_{10}^{2+}, **18**−**4**, at +10.9 kcal/mol is based on a pentagonal bipyramid with three caps oriented to form only two tetrahedral cavities. Then comes D_{2h} tetracapped octahedron **18**−**5** at +18.7 kcal/mol, related to that found experimentally in $Os_{10}H_4CO)_{24}^{2-}$,[14] albeit with a different skeletal-electron count. The final structure with 25 kcal/mol of the global minimum is the C_{3v} tetracapped trigonal prismatic structure **18**−**6** at +21.1 kcal/mol.

Several rather different structures are found for the even more hypoelectronic Ge_{10}^{4+} (Figure 6), and most of these structures are very nonspherical. The lowest-lying structure for Ge_{10}^{4+} is the tricapped pentagonal bipyramid **16**−**1**, which is very similar to structure **18**−**4** for Ge_{10}^{2+}. Next, at +14.5 kcal/mol above **16**−**1**, comes an open C_s structure **16**−**2** with two edge bridges, i.e., two degree 2 vertices (Ge1 and Ge8 in Figure 6). The combination of these two degree 2 vertices with a degree 7 vertex (Ge6 in Figure 6) indicates a very nonspherical structure. Structure **16**−**3** for Ge_{10}^{4+} at +19.0 kcal/mol is generated by edge-sharing and face-sharing of six tetrahedra; its deviation from sphericity is indicated by four degree 3 vertices and two degree 7 vertices. Structure **16**−**4** for Ge_{10}^{4+} at +20.6 kcal/mol is a bicapped cube related to the lowest-lying structure for Ge_{10}^{2+}, **18**−**1**. The remaining structure for Ge_{10}^{4+} within 25 kcal/mol of the global minimum **16**−**1** is **16**−**5** at +24.8 kcal/mol and the rather unsymmetrical C_s polyhedron **18**−**6** with six triangular faces and four quadrilateral faces, two of which are clearly nonplanar.

Most of the computations on the highly charged Ge_{10}^{6+} led to splitting of the 10 germanium vertices into smaller vertex groups, presumably because of the high coulombic repulsion in the highly charged system. This, of course, is the reason for minimizing the charge in the model systems under study. The only connected Ge_{10}^{6+} structure found was an open C_{3v} structure consisting of a tricapped tetrahedron with additional degree 1 vertices attached to the three caps (**14**−**1** in Figure 6).

4. Discussion

4.1 Energies. Figure 7 plots the computed gas-phase energies and free energies in solution for the lowest-energy structures for the Ge_{10}^{z} clusters (z = +6, +4, +2, 0, −2, −4, −6) against their charges. This plot reflects the instability of the isolated highly charged clusters, either positive or negative, and the stabilizing effect of the solvent/environment. The lowest-energy gas-phase global minimum is found for Ge_{10}^{2-}, in accord with its potential three-dimensional aromaticity predicted by the Wade−Mingos rules[23−26] for an n-vertex cluster with $2n + 2$ skeletal electrons.

4.2. Geometry. The two geometries found for Ge_{10}^{z} with several different skeletal-electron counts derive from two different 10-vertex deltahedra (Figure 8), namely the D_{4d} 4,4-bicapped square antiprism with no degree 6 vertices and the C_{3v} *isocloso* 10-vertex deltahedron found in (η^6-arene)-RuB_9H_9 with a single degree 6 vertex. The variations in their

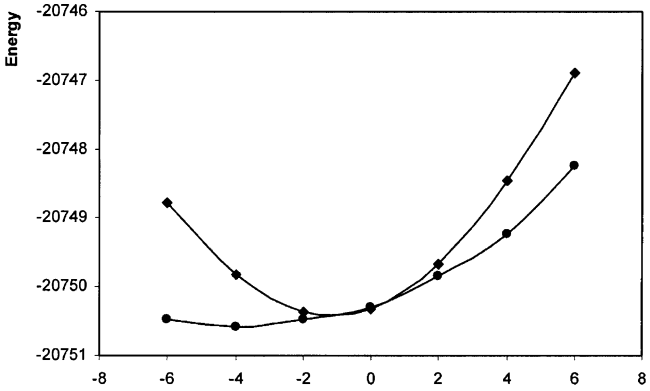

Figure 7. Plot of the total energy of the global minima as a function of charge for the Ge_{10}^{z} (z = −6, −4, −2, 0, +2, +4, +6) clusters; ◆ = gas-phase total energy; ● = total free energy in solution (all in a.u. units).

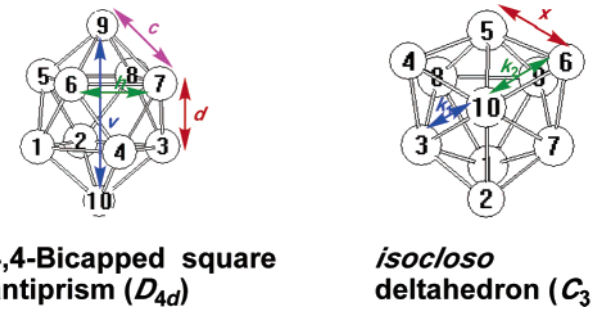

Figure 8. (a) D_{4d} 4,4-bicapped square antiprism; (b)C_{3v} *isocloso* deltahedron.

detailed geometries as a function of skeletal-electron count have been examined, as discussed below.

4.2.1. The D_{4d} Bicapped Square Antiprism. This deltahedral geometry with only degree 4 and 5 vertices is found for the Ge_{10}^{z} clusters (z = −4, −2, 0). The D_{4d} clusters Ge_{10}^{4-} (**24**−**6T**) and Ge_{10} (**20**−**6T**) are found to be triplets consistent with half-filled doubly degenerate frontier orbitals. In addition, a second singlet isomer of Ge_{10} (**20**−**4**) is topologically a 4,4-bicapped square antiprism but is distorted to C_2 symmetry. This pair of Ge_{10} isomers **20**−**4** and **20**−**6T** is apparently analogous to singlet rectangular cyclobutadiene and triplet square cyclobutadiene, respectively, so that the conversion of **20**−**6T** to **20**−**4** can be regarded as a Jahn−Teller distortion. In the 4,4-bicapped square antiprismatic Ge_{10} isomers, the stabilization energy gained by this Jahn−Teller distortion can be estimated at 35.6 − 28.8 = 6.8 kcal/mol from our calculations.

The 24 edges of a 4,4-bicapped square antiprism can be partitioned into three types (Figure 8a), namely the eight edges of the two square faces in the underlying square antiprism (h), the eight edges connecting these two square faces (d), and the eight edges to the two caps (c). Also, the antipodal distance between the two caps (v) is a good measure of the elongation or compression of the 4,4-bicapped square antiprism. However, this distance, as it is obviously not a bonding distance, is not easy to extract from published structural data.

Table 1 lists the relevant distances and distance ratios for the structures derived from the D_{4d} 4,4-bicapped square antiprism computed for the Ge_{10}^{z} clusters as well as experi-

Table 1. Dimensions of the Structures Derived from the 4,4-Bicapped Square Antiprism for Ge_{10}^{z} ($z = -4, -2, 0$) and Related Experimental Data[a]

structure	h (Å)	d (Å)	c (Å)	v (Å)	d/h	c/d	v/h
20−**6T**	2.76	2.60	2.61	5.61	0.94	1.00	2.03
20−**4**	2.66, 2.85	2.53, 2.68	2.49, 2.80	5.71	0.95	1.00	2.08
22−**1**	2.82	2.54	2.59	5.33	0.90	1.02	1.89
$Co_{10}P(CO)_{22}^{2-}$	2.82	2.63	2.59		0.93	0.98	
$B_{10}H_{10}^{2-}$	1.84	1.82	1.70		0.99	0.93	
$B_{10}Br_{10}^{2-}$	1.83	1.82	1.70		1.00	0.93	
24−**6T**	2.76	2.63	2.72	5.96	0.95	1.03	2.16

[a] For structures distorted from ideal D_{4d} symmetry, the averages of the edge sets are taken.

mental structural data. The following observations can be made from these data:

(1) The Ge_{10}^{2-} structure with the 22 skeletal electrons suggested by the Wade−Mingos rules[23−26] is less elongated than the Ge_{10}^{4-} and Ge_{10} structures with 24 and 20 skeletal electrons, respectively, which deviates from the Wade−Mingos rules.

(2) The Jahn−Teller distortion of triplet **20**−**6T** to singlet **20**−**4** does not have a significant effect on the edge-length ratios d/h and c/d if the mean values for the edge lengths h, d, and c are used.

(3) The experimental edge-length ratios for dianion $Co_{10}(\mu_8\text{-P})(CO)_{22}^{2-}$ are in close agreement with those computed for the isoelectronic Ge_{10}^{2-} (**22**−**1**). However, the experimental edge-length ratios for dianions $B_{10}X_{10}^{2-}$ (X = H,[9] Br[29]) deviate significantly from those computed for **22**−**1**. In particular, the edge lengths h and d are essentially identical for $B_{10}X_{10}^{2-}$ (i.e., $d/h = 0.99$ (X = H) to 1.00 (X = Br)), whereas the computed d/h ratio is 0.90 for **22**−**1** and the experimental d/h ratio is 0.93 for $Co_{10}(\mu_8\text{-P})(CO)_{22}^{2-}$.[13] Note also that the dimensions of the $B_{10}X_{10}^{2-}$ anions change very little as hydrogen (X = H) is substituted with bromine (X = Br).

4.2.2. C_{3v} Polyhedra Derived from the *Isocloso* 10-vertex Deltahedron. The other 10-vertex polyhedron found in optimized Ge_{10}^{z} structures with a variety of skeletal-electron counts, i.e., 18−24 skeletal electrons for $z = +2$, 0, −2, and −4, is the C_{3v} *isocloso* deltahedron. This deltahedron with a single degree 6 vertex in addition to three degree 4 and six degree 5 vertices is found in ten-vertex metallaboranes of which (η^6-arene)RuB_9H_9 is the simplest example.

The geometries of the C_{3v} *isocloso* deltahedra can be characterized by the relative lengths of the edges associated with the unique degree 6 vertex (Figure 8b) as was previously done for the C_{2v} edge-coalesced icosahedron in our study of 11-vertex structures.[6] In the case of the 10-vertex C_{3v} deltahedra, the edges associated with the unique degree 6 vertex are of the following two types:

(1) The six v_6-spokes emanating from the degree 6 vertex to the six adjacent vertices. These are partitioned into two sets of three spokes; the length of the longer spoke is designated as k_2 and that of the shorter spoke as k_1. However, in the case of the electron-richest C_{3v} structures, namely **24**−**2** and **22**−**2T**, the length k_2 of the longer spoke is greater than the threshold of 3.00 Å for an edge so that such edges are not drawn in the relevant figures.

Table 2. Geometry Surrounding the Unique Degree 6 Vertex in the C_{3v} *Isocloso* Deltahedra Computed for Ge_{10}^{z} ($z = -4, -2, 0$, and $+2$)

structure	v_6-hexagon (Å)	v_6-spokes (Å)	k_2/k_1
18−**2**	2.71(x)	2.53 (k_2), 2.48 (k_1)	1.02
20−**2**	2.48(x)	2.86 (k_2), 2.54 (k_1)	1.13
(η^6-*p*-cymene)RuB_9H_9		2.31 (k_2), 2.14 (k_1)	1.08
22−**2T**	2.55	3.39 (k_2), 2.46 (k_1)	1.38
24−**2**	2.64	3.36 (k_2), 2.52 (k_1)	1.33

(2) The six edges of the v_6-hexagon formed by the six vertices adjacent to the unique degree 6 vertex. The C_{3v} point group requires these edges to be of the same length, designated as x.

Table 2 summarizes the geometries of the C_{3v} *isocloso* deltahedra studied in this work in terms of the lengths of these edges. The k_2/k_1 ratio of 1.08 found experimentally for (η^6-*p*-cymene)RuB_9H_9 is seen to be closer to that computed for isoelectronic Ge_{10} isomer **20**−**2** than for the C_{3v} structures with other skeletal-electron counts.

4.3. Electron Count vs Geometry: Relevance of the Wade−Mingos Rules. 4.3.1. Three Different Ten-Vertex Deltahedra. The D_{4d} 4,4-bicapped square antiprism with only degree 4 and 5 vertices (Figure 8a) is the most-spherical *closo* deltahedron with 10 vertices.[30] The Wade−Mingos rules[23−26] therefore suggest that this should be the preferred deltahedron for a 10-vertex cluster with $2n + 2 = 22$ skeletal electrons, namely Ge_{10}^{2-}, which is isoelectronic with the well-known[8,9] borane anion $B_{10}H_{10}^{2-}$. Thus, Ge_{10}^{2-} with a D_{4d} 4,4-bicapped square antiprism structure, i.e., **22**−**1** (Figure 1), should exhibit three-dimensional aromaticity[31] and be particularly stable. The skeletal bonding in an n-vertex deltahedron exhibiting such three-dimensional aromaticity can be viewed as a combination of bonds of the following two types:

(1) A single n-center core bond analogous to the π-bonding in benzene but using only two skeletal electrons;

(2) A total of n two-center, two-electron (2c−2e) surface bonds analogous to the σ-bonding in benzene and using $2n$ skeletal electrons.

Consistent with this picture, the D_{4d} 4,4-bicapped square antiprism is computed to be the lowest-energy structure for Ge_{10}^{2-} (**22**−**1**).

A less-spherical 10-vertex deltahedron with a single-degree 6 vertex in addition to degree 4 and 5 vertices and C_{3v} point group symmetry is found in the so-called *isocloso* metallaboranes, of which (η^6-arene)RuB_9H_9 derivatives are the simplest examples. Such deltahedra have 20 rather than the favored 22 skeletal electrons for the D_{4d} 4,4-bicapped square antiprism discussed above. The skeletal bonding in the *isocloso* deltahedra with n vertices has been suggested[32] to consist of n 3c−2e bonds in n faces of the *isocloso* deltahedron, thereby rationalizing the $2n$ skeletal-electron count. In the case of the isoelectronic Ge_{10} (Figure 4), the C_{3v} *isocloso* 10-vertex deltahedral structure **20**−**2** lies only

(29) Einholz, W.; Vaas, K.; Wieloch, C.; Speiser, B.; Wizemann, T.; Ströbele, M.; Meyer, H.-J. *Z. Anorg. Allg. Chem.* **2002**, *628*, 258.

(30) Williams, R. E. *Inorg. Chem.* **1971**, *10*, 210.
(31) King, R. B. *Chem. Rev.* **2001**, *101*, 1119 and references therein.
(32) King, R. B. *Inorg. Chem.* **1999**, *38*, 5151.

3.3 kcal/mol above the likewise C_{3v}, much less spherical 3,4,4,4-tetracapped trigonal prism **20**−**1**.

The third 10-vertex deltahedron found in this work without any degree 3 vertices is the very oblate (squashed) deltahedron found in **24**−**7** with two degree 6 vertices in addition to degree 4 and 5 vertices (Figure 2). The three-dimensional aromaticity model[31] used for **22**−**1** with $2n + 2$ skeletal electrons for $n = 10$ can be adapted to **24**−**7** with two extra skeletal electrons if the 10c−2e core bond in **22**−**1** is split into two 5c−2e core bonds in **24**−**7** because of its extremely nonspherical oblate structure.

4.3.2. Other Electron-Rich Structures. Electron-rich (hyperelectronic) Ge_{10}^{z} clusters, i.e., those with more than 22 skeletal electrons, would be expected by the Wade−Mingos rules to form polyhedral structures with one or more nontriangular faces. Thus, the faces in the experimentally known *nido* structure for $B_{10}H_{14}$ are all triangles except for a single hexagon. However, for the isoelectronic Ge_{10}^{4-}, the C_{2v} decaborane-like structure **24**−**4** (Figure 2) is found to lie +26.3 kcal/mol above the global minimum. Nevertheless, the global minimum structure for Ge_{10}^{4-} (**24**−**1**) is related to the decaborane-like structure **24**−**4** by splitting the hexagonal open face into two quadrilaterals by a transannular bond. The preference of $B_{10}H_{14}$ for a structure similar to that of **24**−**4** with an open hexagon rather than a structure with two quadrilateral faces similar to the global minimum **24**−**1** for Ge_{10}^{4-} may be a consequence of the four extra hydrogen atoms bridging the edges of the hexagonal face in $B_{10}H_{14}$. Such hydrogen atoms, of course, are not present in the isoelectronic Ge_{10}^{4-}.

The even more electron-rich cluster Ge_{10}^{6-} with $2n + 6 = 26$ skeletal electrons would be expected by the Wade−Mingos rules to have an *arachno* structure with two nontriangular faces or one large opening in a polyhedron with otherwise triangular faces. The pentagonal antiprism (e.g., structure **26**−**3** in Figure 3) is computed to be +17.1 kcal/mol above the global minimum **26**−**1** for Ge_{10}^{6-} and is found experimentally in the isoelectronic $Pd@Bi_{10}^{4+}$, assuming the interstitial Pd atom to be a zero-electron donor. The global minimum **26**−**1** computed for Ge_{10}^{6-} is derived from the pentagonal prism rather than the pentagonal antiprism by sliding the top pentagon relative to the bottom pentagon to convert some of the rectangular faces between the two original pentagons to pairs of triangular faces sharing an edge. The resulting rather unsymmetrical C_s polyhedron in **26**−**1** retains two of the five quadrilateral faces of the original pentagonal prism in addition to the two pentagonal faces.

4.3.3. Electron-Poor Structures. Electron-poor (hypoelectronic) deltahedra, i.e., those with less than $2n + 2$ skeletal electrons, can be obtained by capping one or more faces of smaller deltahedra. The overall skeletal-electron count is determined by that required by the central deltahedron with the capping vertex contributing electrons but no bonding orbitals. Thus, octahedra with one or more caps are still expected to have the same 14 skeletal electrons as an uncapped octahedron. Specific examples are found in osmium carbonyl cluster chemistry, such as the capped octahedral $Os_7(CO)_{21}$[33] and the tetracapped octahedral $Os_{10}H_4(CO)_{14}^{2-}$,[14] both of which can be interpreted as having the 14 skeletal electrons required by the central Os_6 octahedron. However, this bonding model can require the availability of more than four valence orbitals at the vertex atoms of the face being capped if there are more than two caps on the faces of a central deltahedron involving faces sharing vertices.

Tetracapped octahedral structures are found for the Ge_{10} and Ge_{10}^{2+} clusters, namely **20**−**5** (Figure 4) and **18**−**5** (Figure 5), respectively. Neither of these clusters has the 14 skeletal electrons required for the central octahedron by the Wade−Mingos rules as tested by the capped octahedral osmium carbonyl clusters mentioned above. However, only two of the four caps in **20**−**5** or **18**−**5**, namely two antipodal caps, can contribute their two skeletal electrons to the central octahedron; this is because these two caps already use all four valence orbitals of all six vertex atoms of the central Ge_6 octahedron by capping all of the atoms of two antipodal faces.

The global minimum **20**−**1** (Figure 4) found for Ge_{10} is another example of an electron-poor 10-vertex deltahedron. In this case, the underlying most-spherical deltahedron is the nine-vertex D_{3h} 4,4,4-tricapped trigonal prism, which has only degree 4 and degree 5 vertices. The 10th Ge vertex caps one of the triangular faces of the underlying trigonal prism, thereby contributing two of the skeletal electrons without contributing any new bonding orbitals.

Another type of capped deltahedron found in electron-poor clusters such as Ge_{10}^{2+} (**18**−**4** in Figure 5) and Ge_{10}^{4+} (**16**−**1** in Figure 6) is a special type of tricapped pentagonal bipyramid. In this 10-vertex deltahedron of ideal C_{2v} symmetry, two symmetry-related faces of the original pentagonal bipyramid are first capped by two new vertices. The tenth vertex is then bonded to the two capping vertices as well as two original vertices of the original pentagonal bipyramid. This arrangement of the 10th vertex eliminates both vertices of degree 3 leading to a 10-vertex deltahedron with four vertices of degree 6 and six vertices of degree 4. This polyhedron is the global minimum (**16**−**1**) for Ge_{10}^{4+} (Figure 6) with the 16 skeletal electrons required by the Wade−Mingos rules for the underlying pentagonal bipyramid.

4.3.4. Mixed Structures. There are some examples of mixed polyhedra in which a hyperelectronic polyhedron with one or more nontriangular faces is capped on one or more of its triangular faces. In this way, the structural features of electron-rich polyhedra having more than $2n + 2$ skeletal electrons are combined with those of electron-poor polyhedra having less than $2n + 2$ skeletal electrons. A simple long-known example of a polyhedron of this type found in osmium carbonyl chemistry is the C_s three-capped square pyramid found in $H_2Os_6(CO)_8$,[34] where one of the triangular faces of a five-vertex nido Os_5 polyhedron, namely the square pyramid, is capped by a sixth vertex.

(33) Eady, C. R.; Johnson, B. F. G.; Lewis, J.; Mason, R.; Hitchcock, P. B.; Thomas, K. M. *Chem. Commun.* **1977**, 385.
(34) McPartlin, M.; Eady, C. R.; Johnson, B. F. G.; Lewis, J. *Chem. Commun.* **1976**, 883.

An interesting example of this type of polyhedron found in the Ge_{10}^{z} clusters studied in this work is structure **26**−**2** (Figure 3) for Ge_{10}^{6-}, which lies only 5.0 kcal/mol above the global minimum **26**−**1**. This structure is derived from a nine-vertex D_{3h} polyhedron with three rhombus faces and eight triangular faces generated from a trigonal prism by capping the three rectangular faces and then removing the vertical edges of the original trigonal prism to give a nine-vertex polyhedron with all degree 4 vertices. With three nontriangular faces, this nine-vertex polyhedron is formally a *hypho* polyhedron, expected by the Wade−Mingos rules to have $2n + 8$ skeletal electrons, which is 26 for $n = 9$. Adding the 10th Ge vertex as a cap to one of the triangular faces of the original trigonal prism provides the final two of the required 26 skeletal electrons for the underlying nine-vertex polyhedron without generating any new bonding orbitals.

5. Summary

The D_{4d} 4,4-bicapped square antiprism found experimentally in $B_{10}H_{10}^{2-}$ and other 10-vertex clusters with 22 skeletal electrons is calculated to be the global minimum by more than 15 kcal/mol for the isoelectronic Ge_{10}^{2-}. The global minima found for electron-rich clusters Ge_{10}^{4-} and Ge_{10}^{6-} are not those known experimentally. However, experimentally known structures for *nido*-$B_{10}H_{14}$ and the pentagonal antiprism of *arachno*-Pd@Bi_{10}^{4+} are found at higher but potentially accessible energies. The global minimum for Ge_{10} is the 3,4,4,4-tetracapped trigonal prism predicted by the Wade−Mingos rules and found experimentally in Ni@Ga_{10}^{10-}. However, the *isocloso* 10-vertex deltahedron found in metallaboranes such as (η^6-arene)RuB_9H_9 derivatives lies only slightly above this global minimum (+3.3 kcal/mol). Structures found for the more electron-poor clusters Ge_{10}^{2+} and Ge_{10}^{4+} include various capped octahedra and pentagonal bipyramids. This study predicts a number of 10-vertex cluster structures that have not yet been realized experimentally but would be interesting targets for future synthetic 10-vertex cluster chemistry involving vertex units isolobal with the germanium vertices used in this work.

Acknowledgment. We are indebted to the National Science Foundation for partial support of this work under Grant CHE-0209857. Part of this work was undertaken with financial support from CNCSIS-Roumania.

Supporting Information Available: Figure S1 (Ge_{10}^{z} initial structures); Table S1 (optimized Ge_{10}^{z} structures with their energies and geometries); Table S2 (HOMO−LUMO energy gaps for the Ge_{10}^{z} optimized structures). This material is available free of charge via the Internet at http://pubs.acs.org.

IC051905M